

# Impacts of the Sahel-Sahara Interface Reforestation on West African Climate: Intra-Annual Variability and Extreme Temperature Events

Ibrahima Diba<sup>1,2</sup>, Moctar Camara<sup>1\*</sup>, Arona Diedhiou<sup>2</sup>

<sup>1</sup>Laboratoire d'Océanographie, des Sciences de l'Environnement et du Climat (LOSEC), UFR Sciences et Technologies, Université A. SECK de Ziguinchor, Ziguinchor, Sénégal

<sup>2</sup>IRD, CNRS, Grenoble INP, IGE, Université Grenoble Alpes, Grenoble, France

Email: \*moctar.camara@univ-zig.sn

**How to cite this paper:** Diba, I., Camara, M. and Diedhiou, A. (2019) Impacts of the Sahel-Sahara Interface Reforestation on West African Climate: Intra-Annual Variability and Extreme Temperature Events. *Atmospheric and Climate Sciences*, 9, 35-61.

<https://doi.org/10.4236/acs.2019.91003>

**Received:** August 15, 2018

**Accepted:** December 10, 2018

**Published:** December 13, 2018

Copyright © 2019 by authors and Scientific Research Publishing Inc.

This work is licensed under the Creative Commons Attribution International License (CC BY 4.0).

<http://creativecommons.org/licenses/by/4.0/>



Open Access

---

## Abstract

The impacts of the reforestation of the Sahel-Sahara interface on the seasonal distribution of the surface temperature and thermal extremes are studied in the Sahel (West African region lying between 11°N and 18°N). We performed a simulation with the standard version of the RegCM4 model followed by another one using the altered version of the same model taking into account an incorporated forest. The impacts of the vegetation change are assessed by analyzing the difference between the two runs. The reforestation may influence strongly the frequency of warm days (TG90P) and very warm days (TX90P) by decreasing it over the reforested zone from March to May (MAM) and the entire Sahel during the June-August (JJA) period. These TG90P and TX90P indices decrease may be due to the strengthening of the atmospheric moisture content over the whole Sahel region and the weakening of the sensible heat flux over the reforested zone. The analysis also shows a decrease of the TN90P indice (warm nights) over the Sahel during the wet season (JJA) which could be partly associated with the strengthening of the evapotranspiration over the whole Sahel domain. The analysis of additional thermal indices shows an increase of the tropical nights over the entire Sahel from December to February (DJF) and during the warm season (MAM). The strengthening of the tropical night is partly associated with an increase of the surface net downward shortwave flux over the reforested zone. When considering the heat waves, an increase (a decrease) of these events is recorded over the southern Sahel during JJA and SON periods (over the whole Sahelian region during DJF), respectively. Changes in latent heat flux appear to be largely responsible for these extreme temperatures change. This work shows that the

---

vegetation change may impact positively some regions like the reforested area by reducing the occurrence of thermal extremes; while other Sahel regions (eastern part of the central Sahel) could suffer from it because of the strengthening of thermal extremes.

## Keywords

RegCM4, Reforestation, Heat Waves, Sahel

---

## 1. Introduction

The sustainability of economic development and living conditions depends on our ability to manage the risks associated with extreme events. Many practical problems require knowledge of the behavior of extreme values. In particular, human health is sensitive to high values of warm extreme. Moreover, a high consensus exists on the reality of global warming across the world [1]. Under this climate warming, heat waves are going to be more frequent and more intense in the next future [2]. Many studies show that mean temperatures have increased due to changes in the daily minimum temperature [3] [4]. The global warming trend is also accompanied by an increase in both frequency and duration of heat waves, which usually are more visible and have larger impacts on ecosystems, economies and societies than the mean changes [5] [6].

It's more difficult for developing countries particularly those of the Sahelian region known for their low income to cope with an increase of heat waves compared to developed countries of Europe where capacities in mitigation and adaptation are considered to be more efficient. For example in 2010, Niger has experienced episodes of extreme heat that it hadn't known for the last 130 years and such thermal extremes had many impacts on agriculture and morbidity of the population [7].

Furthermore, the 21<sup>st</sup> century global warming due to anthropogenic forcing will be strong over Africa, which is likely to increase the number and duration and amplitude of heat waves, especially in arid and semi-arid regions of the Sahel [2] [8] [9] [10].

Likewise, Fontaine *et al.* [11] showed a significant warming (1°C to 3°C) for the period 1979-2011 over Sahara and Sahel. These authors associated the warming trend with more frequent warm temperatures (exceeding the 90th percentile) as well as higher frequencies and longer durations of heat waves.

Understanding the heat waves characteristics and the associated physical mechanisms is highly needed to develop adequate mitigation and adaptation strategies. Studies by [12] have shown that the low-frequency variations are the main signature of the global warming and that the high-frequency variations are dominated by the delayed impact of El Nino Southern Oscillation events over West Africa, with warm temperature anomalies tending to follow warm ENSO events. Oueslati *et al.* [13] also documented the link between Heat Waves (HWs)

characteristics in the Sahel and the associated physical mechanisms. They pointed out that the atmospheric circulation plays an important role in sustaining warming by advecting moisture from the Atlantic Ocean and the Guinean coasts into the Sahel.

Moreover, several studies [14]-[20] have investigated the impacts of land cover characterization on West African climate. This land cover characterization is increasingly recognized as an important forcing of local [21] [22], regional [23] and global climate [24] [25]. Mahmood *et al.* [26] argued that such influences are established through biogeochemical and biogeophysical interactions involving the trace gas exchanges such as carbon, hydrological processes as well as exchange of heat, and momentum fluxes through the atmospheric boundary layer. Xue *et al.* [27] showed that desertification increases surface temperature and affects both the intensity and spatial extent of precipitation and the associated circulation over West Africa. According to them the surface temperature increase is related to the increase of the albedo and the decrease of evaporation. Furthermore, Zheng and Eltahir [28] found that the West African monsoon circulation and rainfall variability are more sensitive to deforestation than to desertification. Using a regional climate model (RegCM3). Studies by [29] simulated an increase of the intensity of the African Easterly Jet (AEJ) core with deforestation option. They concluded that such increase reduce the northward transport of moisture needed for precipitation over West Africa. The impacts of the reforestation on the characteristics of heatwaves over West Africa during the near future (2030-2060) under the RCP 4.5 greenhouse gaz scenario have been investigated by [20]. Their results indicate that the forestation may increase the projected number of heat waves events over the savannah zone and decrease them over the Sahel and along the Guinea coast.

All these pioneering studies cited above helped to better understand the heat waves characteristics and associated mechanisms in West Africa. They also emphasized the key role of land vegetation cover changes on the variability of West African climate. However, none of these studies have attempted to investigate the impacts of the reforestation at the Sahel-Sahara interface (which is the transition region between the semi-arid region called Sahel and the Sahara desert) on the West African daily extreme temperature events for the present-day. Then the necessity to take into account the impacts of a possible change of land cover properties (especially changes in vegetation) on the occurrence of such extremes becomes an important topic to investigate. This work is oriented in this perspective. It investigates the impacts of the reforestation of the Sahel-Sahara interface on the annual distribution of surface temperature and extreme heat temperatures over the Sahel region as well as the atmospheric factors associated to this variability using the International Center for Theoretical Physics (ICTP) regional climate model RegCM4. As the reforestation activities could increase or decrease extremes events, there is a need for detailed studies on how the reforestation may alter the present climate. The overall question addressed here, is to know which Sahel sub-regions could benefit or suffer when reforesting the Sa-

hel-Sahara interface as proposed in the Great Green Wall (GGW) project. The GGW project is an African initiative which goal is to green a strip of land extending from Senegal to Djibouti in order to fight against the desertification and climate change consequences

(<https://www2.uncd.int/actions/great-green-wall-initiative>). The paper is structured as follows. Section 2 describes the experimental design, methods and the thermal indices used following the guidelines of the Expert Team on Climate Change Detection and Indices (ETCCDI). Section 3 presents the results and the discussion. Finally in Section 4, concluding remarks are provided.

## 2. Model Description, Experimental Design and Data Used

### 2.1. Model Description

We used the latest version of the regional climate model RegCM4.5 developed at the Abdu Salam International Center for Theoretical Physics (ICTP) as described in [30]. The RegCM4.5 is a hydrostatic, compressible, sigma-p vertical coordinate model run on Arakawa B-grid which includes various options of physics parameterizations. The model has 18 levels in the vertical and is based on the hydrostatic dynamical core of the National Centre for Atmospheric Research/Pennsylvania State University's mesoscale meteorological model Version 5 (NCAR/PSU's MM5; [31]). In RegCM4, the radiative transfer calculations are carried out with the radiative transfer scheme of the Community Climate Model (CCM3) [32], as implemented by [33]. This scheme includes calculations for the short-wave and infrared parts of the spectrum, including both atmospheric gases and aerosols.

For our experiments, interactions between the land surface and the atmosphere are described using the Biosphere Atmosphere Transfer Scheme (BATS1E; [34]), while the scheme of [35] is used to represent fluxes from ocean surfaces. Resolvable precipitation processes are treated with the subgrid explicit moisture scheme (SUBEX) of [36], which is a physically based parameterization including subgrid-scale cloud fraction, cloud water accretion and evaporation of falling rain drops. The model has been used previously for various studies over different African domains [15] [37] [38] [39].

### 2.2. Experimental Design

The Land surface processes are represented by the Biosphere Atmosphere Transfer Scheme 1E (BATS1E) as described in [34] whereas the nonlocal vertical diffusion scheme of Holstag *et al.* [40] model is used for the parameterization of the planetary boundary layer. We used a mixed convection schemes, those of [41] with the closure of [42] over land areas and [43] over ocean. Two experiments (models runs) are integrated over the West African domain (**Figure 1**) from November 2002 to December 2009 as in [18]. The first two months are considered as spin-up time and are not included in the analysis. The simulations are forced by the ERA-Interim reanalysis [44] [45] at the initial and lateral

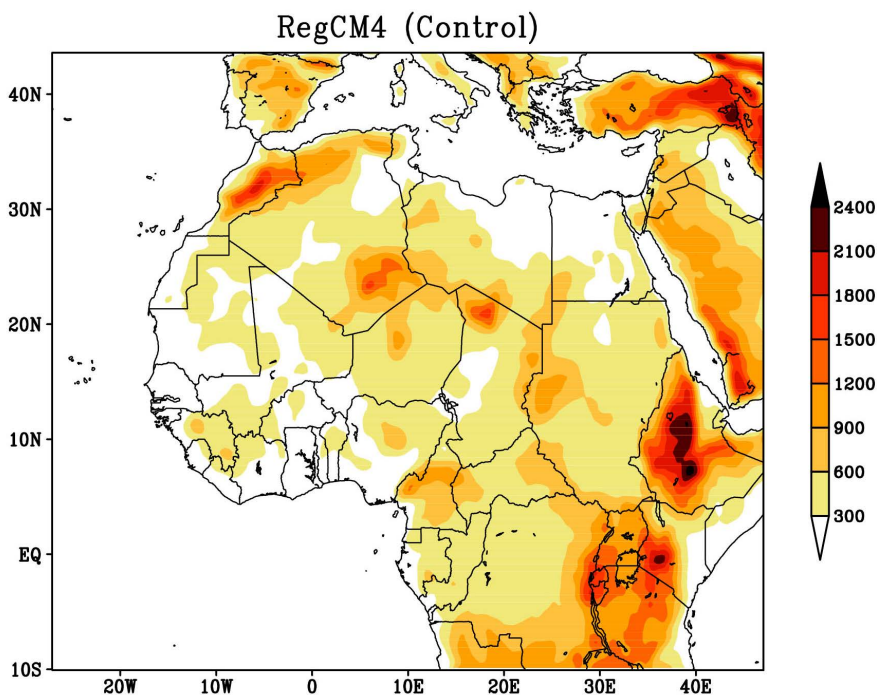


**Figure 1.** Topography of the simulation domain (West Africa) and the orographic regions from the RegCM4 model.

boundaries and are carried out at a spatial resolution of 50 km. The simulation domain (**Figure 1**) shows the orographic regions: Fouta Jallon Mountains (FJM), Jos Plateau (JP) and Cameroon Highlands (CH). The simulations are performed using two different land cover patterns shown in **Figure 2**. In the control (CTR) experiment (**Figure 2(a)**), we used the default land cover pattern (vegetation) of West Africa provided by the standard version of the RegCM4 model. The second experiment (named RegCM4\_REFORESTATION) is identical to the first with the exception that the land cover patterns over the region between 15°N and 20°N which is a combination of grass (15°N - 16°N), semi-desert (16°N - 18°N), and desert (18°N - 20°N) is changed to forest/field mosaic (**Figure 2(b)**). The different types of land cover patterns used are shown in **Table 1**. In response to this vegetation cover change (forest/field mosaic), several physical parameters, such as albedo, leaf area index and the roughness length are significantly modified as shown by **Table 2**. These parameters make the difference between the standard version of the RegCM4 model and the reforested one (**Figure 2**).

### 2.3. Data and Methods

The observed monthly mean surface temperatures of Climate Research Unit (CRU) TS3.22 [46] data are used to validate the model surface temperature output. These gridded TS (time-series) data cover the period 1901-2013. These datasets are calculated on high resolution of  $0.5 \times 0.5$  grids, which are based on an archive of monthly mean surface temperatures provided by more than 4000 weather stations distributed around the world. Model simulations are initialized

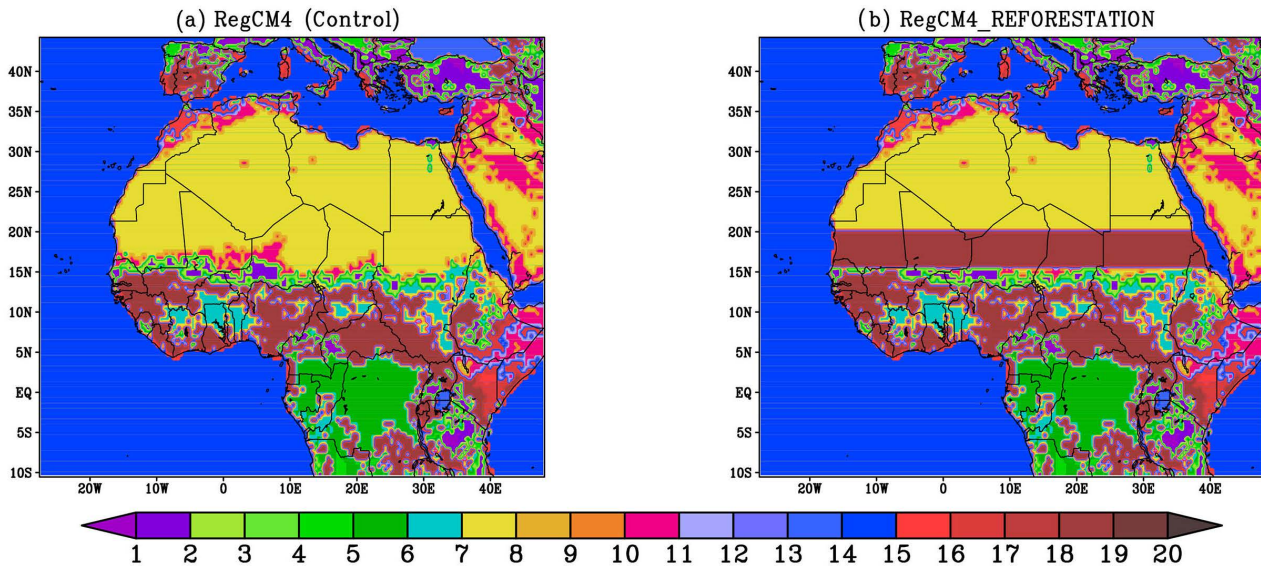


**Figure 2.** Distribution of land cover types used in this study: (a) the standard version of RegCM4 model and (b) the reforested one RegCM4\_REFORESTATION. The reforested zone (between 15°N - 20°N).

**Table 1.** Land cover types/vegetation classes used in this study. NB: the values below indicate the type of land cover used in this study which can be found in the legend of **Figure 2**.

- 1) Crop/mixed farming
- 2) Short grass
- 3) Evergreen needle leaf tree
- 4) Deciduous needle leaf tree
- 5) Deciduous broadleaf tree
- 6) Evergreen broadleaf tree
- 7) Tall grass
- 8) Desert
- 9) Tundra
- 10) Irrigated crop
- 11) Semi-desert
- 12) Icecap/glacier
- 13) Bog or marsh
- 14) Inland water
- 15) Ocean
- 16) Evergreen shrub
- 17) Deciduous shrub
- 18) Mixed woodland
- 19) Forest/field mosaic
- 20) Water and land mixture

**Table 2.** Land cover characteristics used in the study.

Parameters	Short Grass	Tall Grass	Desert	Semi-Desert	Forest
Max fractional vegetation cover	0.80	0.80	0.00	0.35	0.80
Vegetation albedo for wave lengths < 0.7 $\mu\text{m}$	0.10	0.08	0.20	0.17	0.06
Vegetation albedo for wave lengths > 0.7 $\mu\text{m}$	0.30	0.30	0.40	0.34	0.18
Difference between max fractional Vegetation cover and cover at 269 K	0.1	0.0	0.2	0.0	0.4
Roughness length (m)	0.05	0.10	0.05	0.10	0.30
Min stomatal resistance (s/m)	60	60	200	150	120
Max Leaf Area Index	2	6	0	6	6
Min Leaf Area Index	0.5	0.5	0	0.5	0.5
Stem (dead matter area index)	4.0	2.0	0.5	2.0	2.0
Root zone soil layer depth (mm)	1000	1000	1000	1000	2000
Soil texture type	6	6	3	5	6
Soil color type	3	4	1	2	4

and driven by the ERA-Interim reanalysis (spatial resolution of  $1.5 \times 1.5$ ; [44] [45]). A reanalysis data is the results of the combination of the outputs of a numerical weather model with all available observations data. The ERA-Interim reanalysis are available from 1979 to the present and have been used previously for various studies [47] [48] [49] [50] because of their good ability to reproduce the main components of the West African monsoon system [51] [52]. In this study, we investigate the impact of the Sahel-Sahara interface vegetation change (reforestation) on the seasonal variability of extreme temperatures. We use seven (7) warm indices recommended by the World Meteorological Organization (WMO) Expert Team on Climate Change Detection and Indices [53] summarized in **Table 3** known for their serious threat to human health. The work offers a comprehensive analysis of the potential impacts of the reforestation of the Sahel-Sahara interface on the spatial distribution of surface temperature and thermal extremes over the Sahel.

### 3. Results and Discussions

#### 3.1. Model Validation

We first validated the simulations of the standard version of the RegCM4 model before studying the impacts of the reforestation on the seasonal distribution of the surface temperature and thermal extremes by comparing the mean surface temperature simulated by the model with the CRU observations data. **Figure 3** represents the seasonal distribution of mean surface temperature averaged from 2003 to 2009 for the CRU TS3.22 data, the standard version of RegCM4 model and their difference. From December to February (DJF), the CRU observations and the RegCM4 model (**Figure 3(a)**; **Figure 3(b)**) show a minimum of surface

**Table 3.** Summary of the seven 7 thermal indices used.

Index	Index abbreviate	Unit
Percentage of days with daily Tm (mean surface temperatures) > 90th percentile on running 5 day windows (= warm days)	TG90P	%
Percentage of days with daily TX (maximum temperatures) > 90th percentile on running 5 day windows (= very warm days)	TX90P	%
Percentage of nights with daily minimum temperatures TN >90th percentile on running 5 day windows (= warm nights)	TN90P	%
«Hot Days: “HtD”» (= days with TX > 35°C)	HtD	Count in day
«Tropical Nights: “TrN”» (= nights with TN > 20°C)	TrN	Count in day
Number of Heat Waves	HW	Count in day
Warm spell days	WSD	Length in day

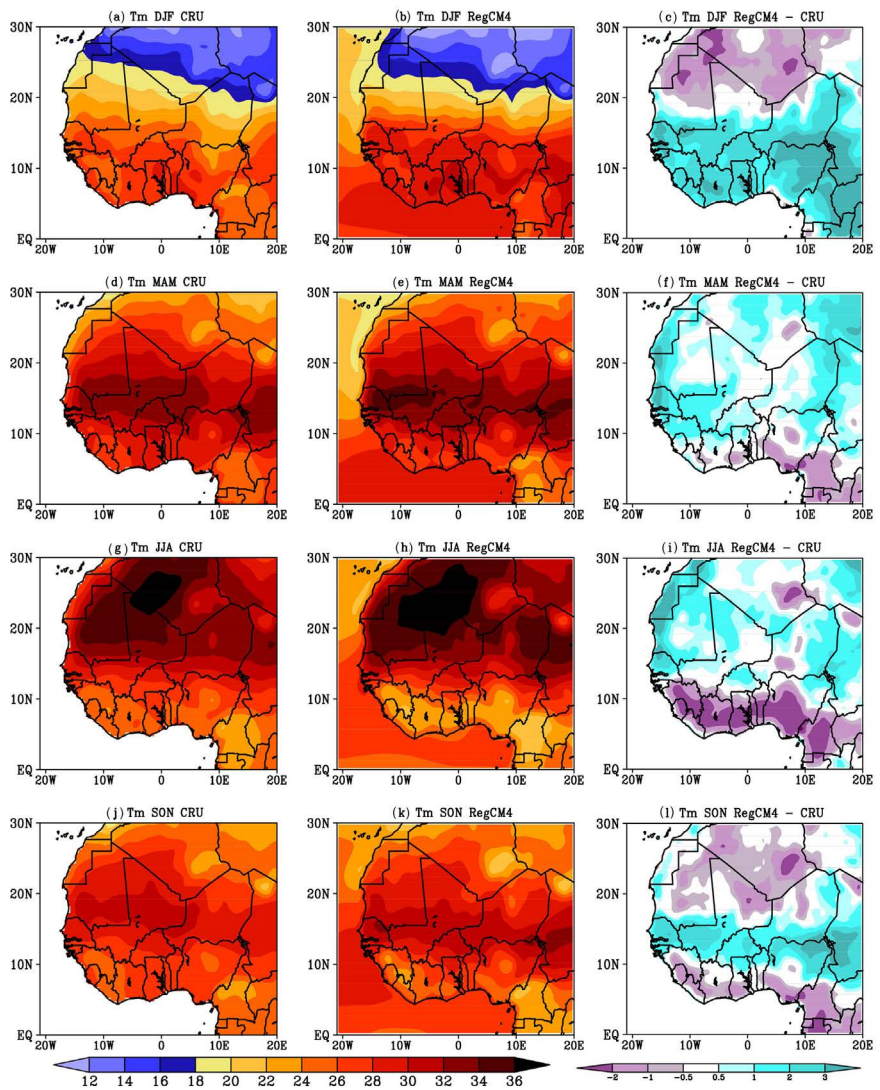


**Figure 3.** Seasonal average temperature (°C) from 2003 to 2009 over West Africa for CRU TS3.22 data, RegCM4 and RegCM4-CRU TS3.22 data.

temperature over the Sahara desert (below 18°C) and the maxima temperature (above 30°C) over the Sahel. The RegCM4 model underestimated (overestimated) the surface temperature over the Sahara desert (over the Sahel), respectively during this same period. Higher values (above 32°C) of surface temperature are observed by CRU and simulated by RegCM4 over the Sahel from March to May (MAM); the MAM period is considered as the Sahel warm season. During the summer season (June-August; JJA), the CRU observations data (**Figure 3(g)**) show a North-South gradient with higher surface temperature values (above 34°C) recorded over the western part of the Sahara desert and coldest surface temperatures over the orographic regions (Guinean Highlands (10°N, 13°W), Jos plateau (10°N, 7.5°E) and Cameroon Mountains (6°N, 12°E)). RegCM4 (**Figure 3(h)**) exhibits this North-South gradient and a maximum (above 34°C) around the area of the Saharan Heat Low (SHL) centered over 25°N (northern Sahel) partly linked to the onset of the rainy season over the Sahel [54] [55]. This maximum (above 34°C) migration initiates a progressive increase in meridional surface air temperature gradient that strengthens and shifts northward the features triggering and maintaining the West African Monsoon which ultimately favors intense convection and precipitation in the Sahel [36] [56] [57]. The model well reproduces the minima (below 24°C) over the orographic regions from September to November (**Figure 3(k)**), demonstrating its capability to capture the fine-scale features over regions of steep orography. The Gulf of Guinea experiences relatively lower and uniform temperatures with a maximum of 28°C during MAM associated partly with the pre-monsoon season and a minimum of 24°C during the peak of the monsoon season (JJA). A cold bias (below -2°C) prevails over the Guinean coast during MAM, JJA and SON. The smallest bias (below -2°C) occurs over the northern Sahel and the Sahara desert during DJF. However a warm bias (around 2°C) is simulated over the Sahel and the western part of the Sahara desert during MAM and JJA periods.

Globally, the analysis reveals that the cold biases are more visible in the desert areas and the coastlines along the Gulf of Guinea.

It is difficult to determine the causes of the Regional Climate Models (RCMs) temperature biases [58]. However, the previous authors indicate that the main driver for the surface temperature biases in RegCM4 simulations is latent heat rather than radiative fluxes. Overall, some authors like [30] [59] showed that the cold bias simulated by the regional climate models could partly originate from an inaccurate representation of surface albedo, vegetation distribution and partitioning of net solar and longwave radiation into latent and sensible heat. However, the low bias in **Figure 3** especially over the Sahel region shows the ability of the RegCM4 model to simulate the West African surface temperature patterns. The next step is to evaluate the impacts of the reforested area on the seasonal distribution of the surface temperature and extreme heat temperatures over the Sahel band as well as the atmospheric factors associated to this variability.

### 3.2. Impacts of Reforestation on Thermal Extremes

The first lines of this part are devoted to the analysis of some atmospheric parameters necessary to a better interpretation of the seasonal distribution of thermal extremes over the Sahel region (West African region lying between 11°N and 18°N). **Figure 4** shows the evapotranspiration averaged from 2003 to 2009 for RegCM4 model (control case) (top) and the difference between both runs (down). The evapotranspiration decreases from the North to the South for all seasons. The strongest values (above 4  $\text{cg}/\text{m}^2/\text{s}$ ) are reached during the summer season (JJA) over the southern Sahel. The smallest values (below 1.5  $\text{cg}/\text{m}^2/\text{s}$ ) are found over the northern Sahel for all seasons. The difference between the reforested run and the control simulation shows an increase of the evapotranspiration over the entire Sahel domain for all seasons with strong values (above 1.2  $\text{cg}/\text{m}^2/\text{s}$ ) during the summer season (JJA). This increase is consistent to the strengthening of the atmospheric moisture content integrated in the lower layers (between 1000 and 850 hPa) (Figure not shown) over the whole Sahel domain. A

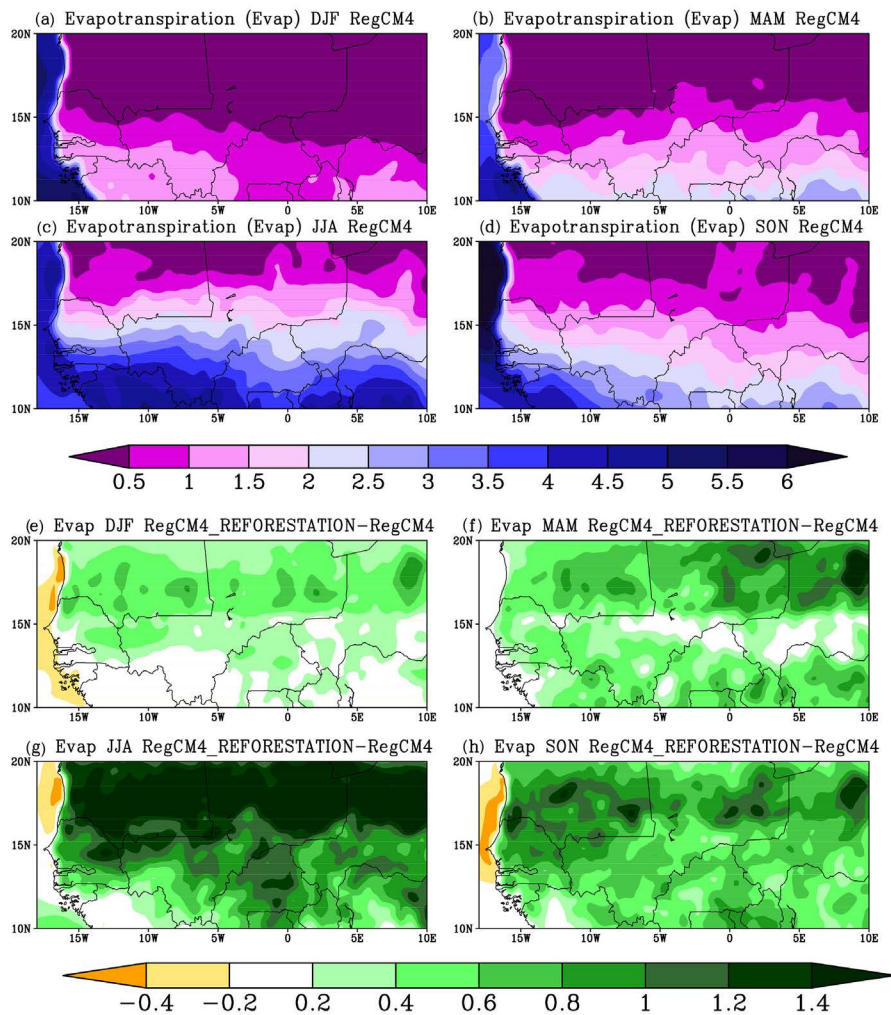


**Figure 4.** Evapotranspiration ( $\text{cg}/\text{m}^2/\text{s}$ ) averaged from 2003 to 2009 over the Sahel: (top) RegCM4, (down) difference between RegCM4\_REFORESTATION and RegCM4.

small decrease of the evapotranspiration ( $-0.4 \text{ cg/m}^2/\text{s}$ ) is recorded in the Atlantic Ocean during DJF, JJA and SON.

The sensible heat flux averaged from 2003 to 2009 for RegCM4 (top) and the difference between the two runs (down) is displayed in **Figure 5**. The standard version of the RegCM4 model simulates the maxima of sensible heat flux ( $>70 \text{ W}\cdot\text{m}^{-2}$ ) over the southern part of the Sahel during DJF, over the entire Sahel region during the warm season (MAM), over the northern Sahel during the summer season (JJA) and over a latitudinal band located between  $12^\circ\text{N}$  and  $18^\circ\text{N}$  during SON. The reforestation tends to decrease the sensible heat flux during MAM, JJA and SON over the southern Sahel with strong values ( $>-20 \text{ W}\cdot\text{m}^{-2}$ ) during the summer season (JJA) and to increase it over the reforested zone especially during DJF, MAM and SON (**Figure 5**).

The latent heat flux averaged from 2003 to 2009 for RegCM4 (top) and the difference between both runs (down) is displayed in **Figure 6**. The standard version of the RegCM4 model shows a dipolar structure with the maxima

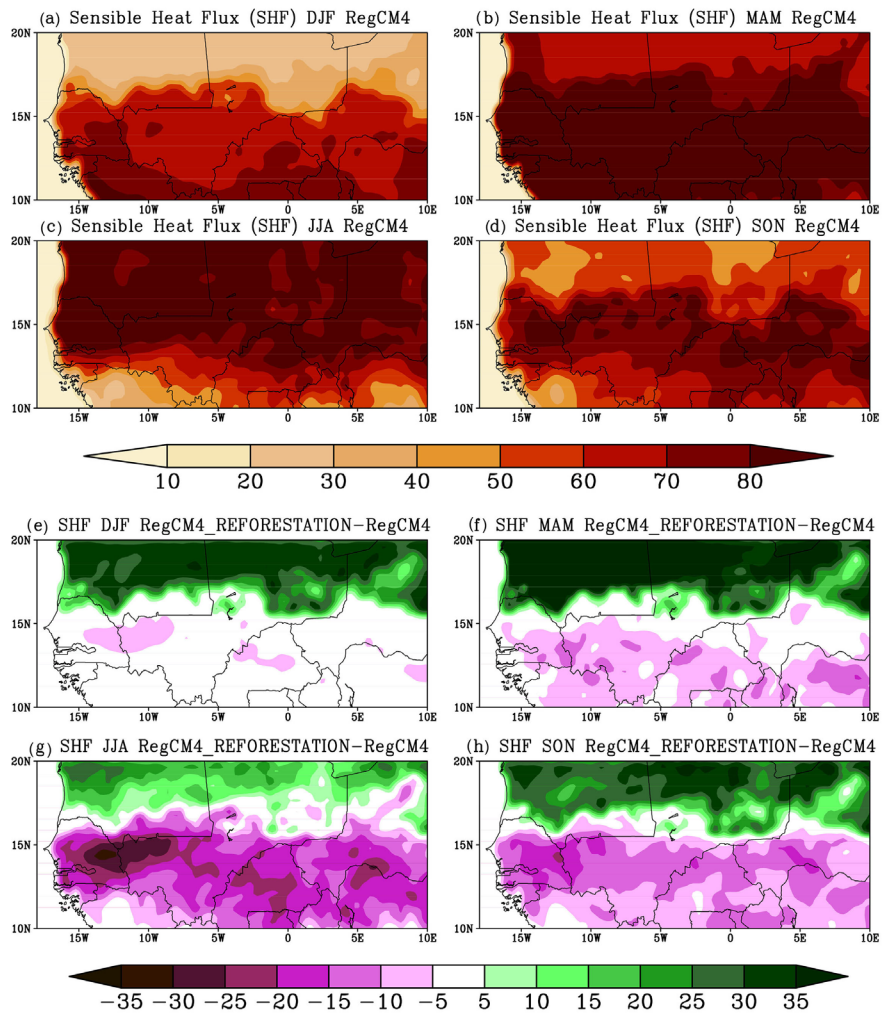


**Figure 5.** Sensible heat flux ( $\text{W}\cdot\text{m}^{-2}$ ) averaged from 2003 to 2009 over the Sahel: (top) RegCM4, (down) difference between RegCM4\_REFORESTATION and RegCM4.

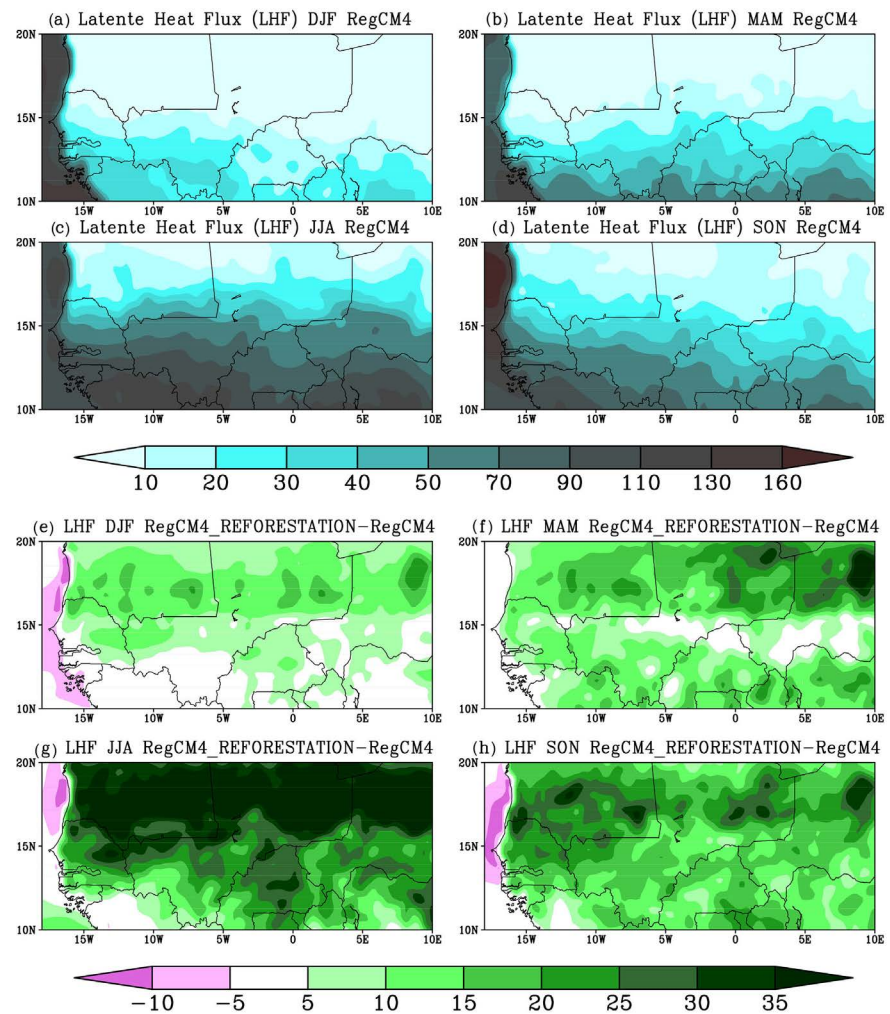


**Figure 6.** Latent heat flux ( $\text{W}\cdot\text{m}^{-2}$ ) averaged from 2003 to 2009 over the Sahel: (top) RegCM4, (down) difference between RegCM4\_REFORESTATION and RegCM4.

( $>50 \text{ W}\cdot\text{m}^{-2}$ ) located over the southern Sahel and the ocean and the minima ( $<20 \text{ W}\cdot\text{m}^{-2}$ ) over the northern Sahel for all seasons. The reforestation tends to increase the latent heat flux during DJF over the northern Sahel and over the entire Sahel domain during JJA, MAM and SON with strong values ( $>30 \text{ W}\cdot\text{m}^{-2}$ ) over the reforested zone during the summer season JJA (Figure 6). The sensible heat flux decrease by  $20 \text{ W}\cdot\text{m}^{-2}$  (Figure 5) over the southern Sahel during the summer season (JJA) appears partly as an increase in the latent heat flux (Figure 6) over the same zone and the same season.

The analysis of the surface net upward longwave flux (Figure 7) shows that the standard version of RegCM4 model simulates stronger values ( $> 90 \text{ W}\cdot\text{m}^{-2}$ ) over the northern Sahel for all seasons. Likewise, high values ( $> 110 \text{ W}\cdot\text{m}^{-2}$ ) are found over the entire Sahel region from December to February. A decrease of the net surface heat flux is captured during the rainy season (JJA). The impact of the reforestation is to decrease the upward longwave flux over the entire Sahel for all seasons with strong values ( $-15 \text{ W}\cdot\text{m}^{-2}$ ) during the summer season (JJA)

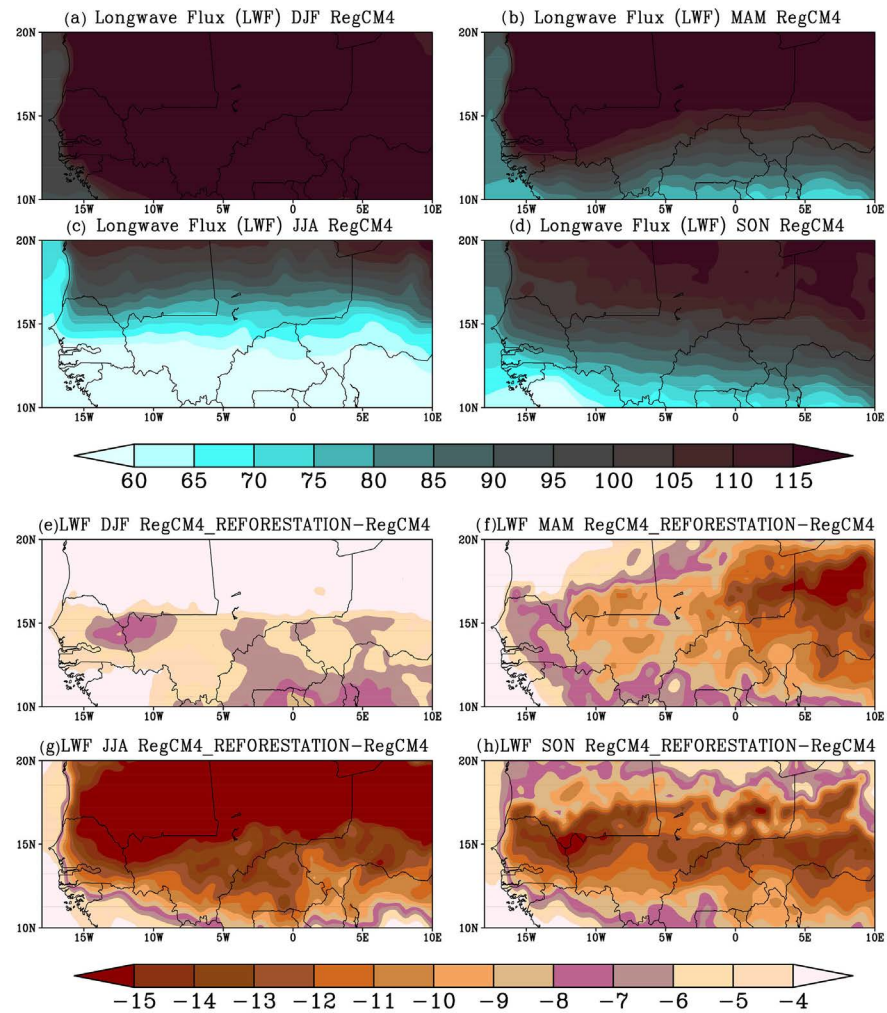


**Figure 7.** Surface net upward longwave flux ( $\text{W}\cdot\text{m}^{-2}$ ) averaged from 2003 to 2009 over the Sahel: (top) RegCM4, (down) difference between RegCM4\_REFORESTATION and RegCM4.

over the reforested area and during the warm period (MAM) over the eastern Sahel. This decrease appears partly as an increase in the sensible heat flux (Figure 6) over the reforested zone.

Figure 8 shows the surface net downward shortwave flux ( $\text{W}\cdot\text{m}^{-2}$ ) averaged from 2003 to 2009 for the RegCM4 model (top) and the difference between the two runs (down). The standard version of RegCM4 model shows the maxima ( $>180 \text{ W}\cdot\text{m}^{-2}$ ) of shortwave flux over the western Sahel and the Atlantic Ocean for all seasons. The higher values ( $>230 \text{ W}\cdot\text{m}^{-2}$ ) are found over the western and eastern parts of the Sahel during the warm season (MAM). The reforestation tends to decrease the surface net downward shortwave flux over the southern Sahel and to increase it over the reforested zone for all seasons.

Figure 9 shows the percentage of days with the daily mean surface temperature greater than the 90th percentile of the daily mean surface temperatures (TG90P) averaged from 2003 to 2009 for RegCM4 model (top) and the difference

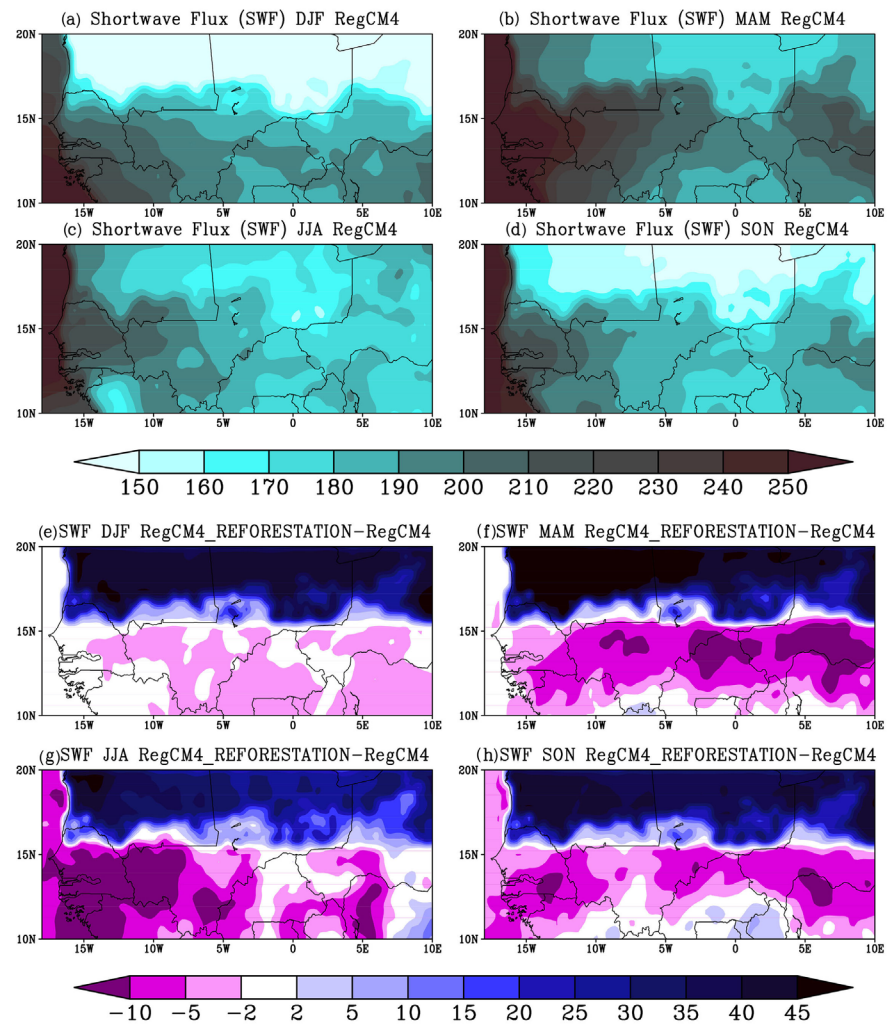


**Figure 8.** Surface net downward shortwave flux ( $\text{W}\cdot\text{m}^{-2}$ ) averaged from 2003 to 2009 over the Sahel: (top) RegCM4, (down) difference between RegCM4\_REFORESTATION and RegCM4.

between both runs (down). RegCM4 experiment exhibits lower frequency (<6%) of the TG90P indice over the Central Sahel from December to February. The maximum of the TG90P indice (>22%) is recorded over the northern Sahel from June to August, over the eastern Sahel from September to November and over the entire Sahel during the MAM period. Between 20% and 24% of the warm days occurred during JJA over the northern Sahel and during MAM over most part of the Sahel. The difference between the two simulations of the model shows that the reforestation could influence strongly the frequency of the TG90P. This indice decreases over the reforested zone during the warm period (MAM), over the western and eastern Sahel during SON and over the entire Sahel during the summer period (JJA).

We also computed and displayed in **Figure 10** the TX90P indice (very warm days). RegCM4 experiment exhibits lower frequency (<6%) of the very warm days over the northern part of the Central Sahel during DJF, over the western

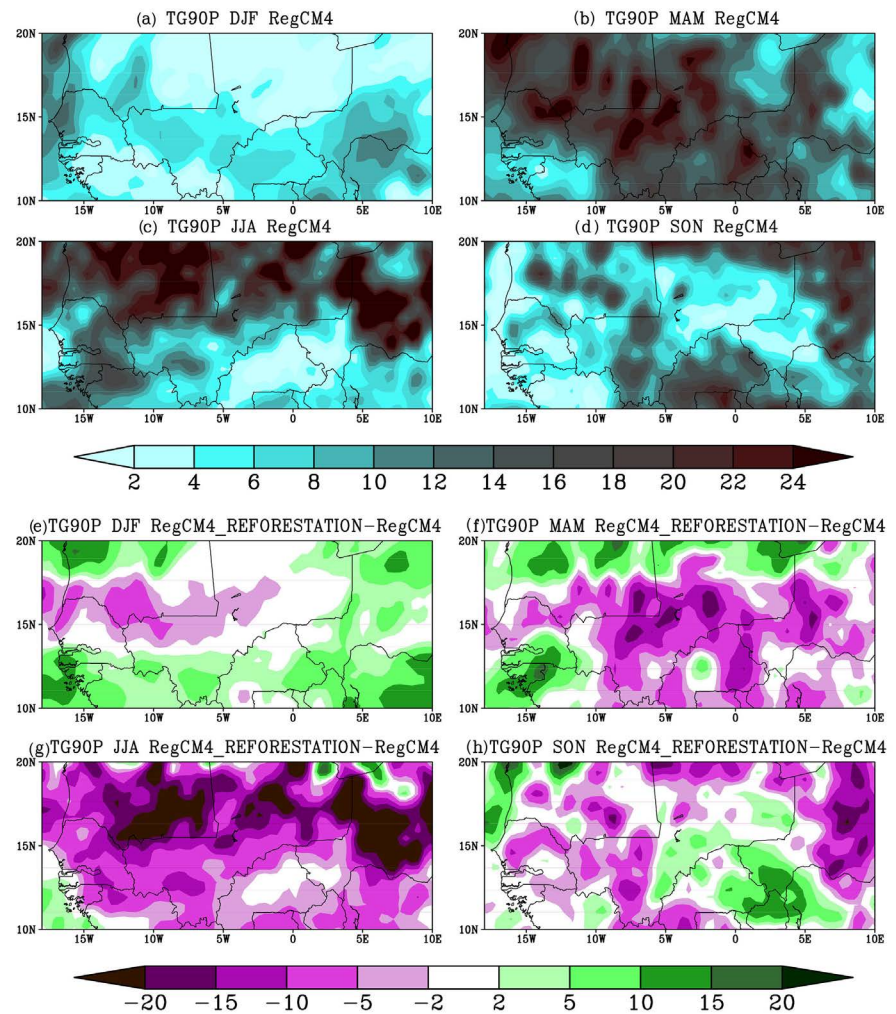


**Figure 9.** Percentage of days with a daily mean surface temperature greater than the 90th percentile of the daily mean surface temperatures (TG90P) averaged from 2003 to 2009 over the Sahel: (top) RegCM4, (down) difference between RegCM4\_REFORESTATION and RegCM4.

Sahel and the North-East part of the Sahel from September to November (SON) and over the southern Sahel during the summer season (JJA). Overall, the maximum of the TX90P indice ( $>18\%$ ) is recorded over the western Sahel during JJA, over the South-East part of the eastern Sahel during SON and over the entire Sahel during the warm season (MAM). Between 18% and 20% of the very warm days occurred during the warm season (MAM) over the northern Sahel in coherence with [12]. The difference between the two runs shows a decrease of the TX90P indice over the reforested zone during MAM, over the western and eastern Sahel during SON and over the entire Sahel during the summer period (JJA). The TG90P and TX90P indices decrease may be due partly to an increase of the atmospheric moisture content over the entire Sahel region (Figure not shown). These indices decrease are also associated to a weakening of the sensible heat flux over the reforested area and over the entire Sahel region during JJA (Figure 5).

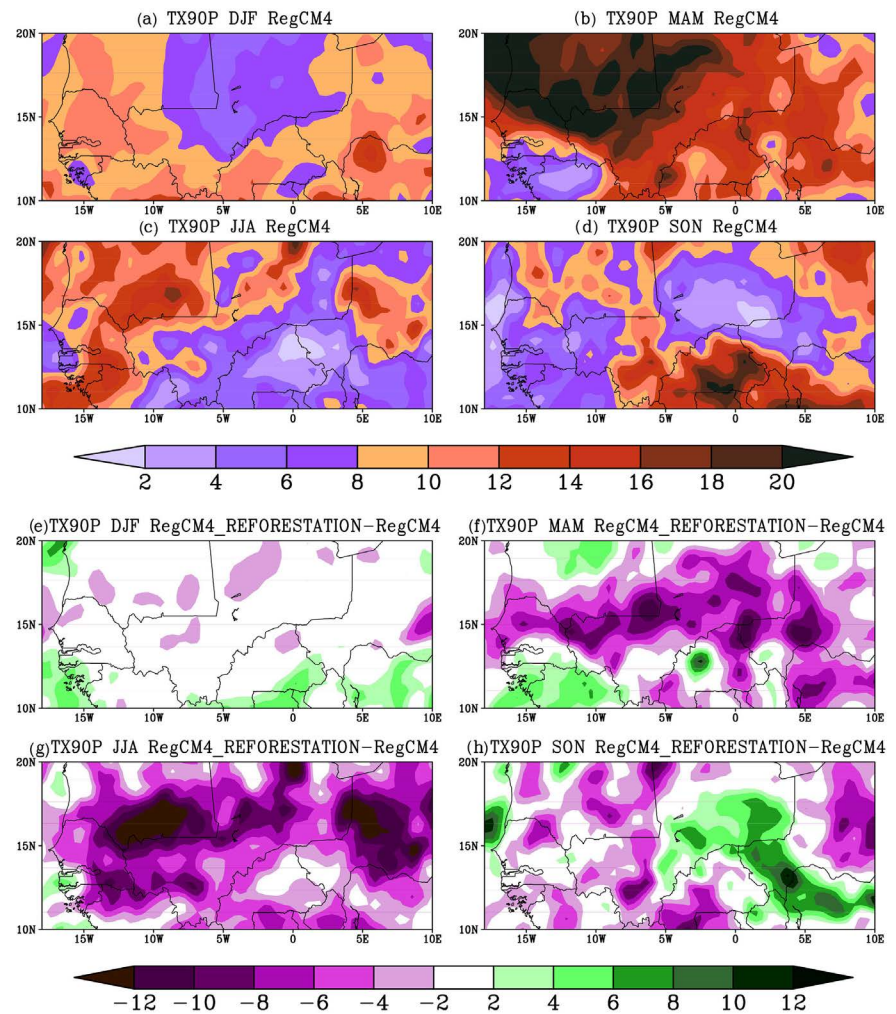


**Figure 10.** Percentage of days with a daily maximum temperature greater than the 90th percentile of the daily maximum temperatures (TX90P) averaged from 2003 to 2009 over the Sahel: (top) RegCM4, (down) difference between RegCM4\_REFORESTATION and RegCM4.

**Figure 11** shows the frequency of warm nights (TN90P) averaged from 2003 to 2009 for the standard version of RegCM4 model and the difference between the two runs. The TN90P indice is relatively weak (<9%) during DJF over the entire Sahel (**Figure 11(a)**) and during SON over the Atlantic Ocean especially over the Guinean coast, Dakar and western part of Mali (**Figure 11(d)**). This may be due to the cooling effect of the sea, including the Canary upwelling during this period. The TN90P indice is longer (>21%) over the western and Central Sahel during MAM and over the northern Sahel (**Figure 11(c)**) during JJA. The difference between the two runs shows a decrease of the TN90P indice over the northern Sahel during DJF, over the northern and Central Sahel during MAM period, over the western and eastern Sahel during SON and over the entire Sahel during the wet season (JJA). This TN90P indice decrease could be associated partly to the increase of the evapotranspiration over the entire Sahel band (**Figure 4**).

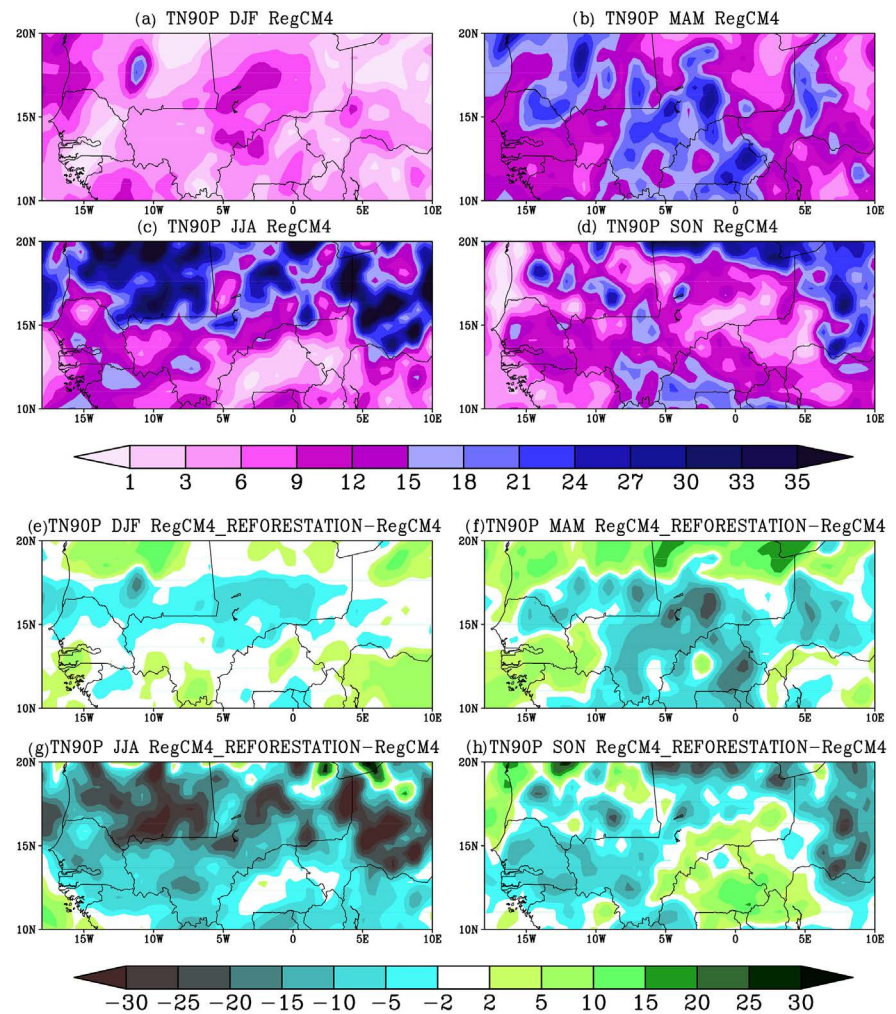


**Figure 11.** Percentage of days with a daily minimum temperature greater than the 90th percentile of the daily minimum temperatures (TN90P) averaged from 2003 to 2009 over the Sahel: (top) RegCM4, (down) difference between RegCM4\_REFORESTATION and RegCM4.

Two absolute extremes which are relevant for impacts studies over the Sahelian region have been considered: the frequency of very hot days (HtD: days with  $TX > 35^{\circ}\text{C}$ ) and the tropical nights (TrN: nights with  $TN > 20^{\circ}\text{C}$ ) as considered in [12]. The analysis of the seasonal variability of the hot days (Figure 12) shows that generally the longer hot days ( $>60$  days) are recorded over the northern part of the Sahel during DJF, MAM, JJA except during SON where we found stronger values ( $>70$  days) over the eastern part. The strongest values ( $>80$  days) are reached during the warm season (MAM) over the entire Sahel linked to a larger amount of the surface net downward shortwave flux (Figure 8) during this dry season. The shorter values ( $<20$  days) of this indice are localized along the coast and over the Atlantic Ocean. This may be due partly to the sea surface temperature cooling. The difference between the two versions shows a decrease of the HtD over the entire Sahel for all seasons. This is partly associated to a decrease of the sensible heat flux over the reforested zone (Figure 5) and an increase of

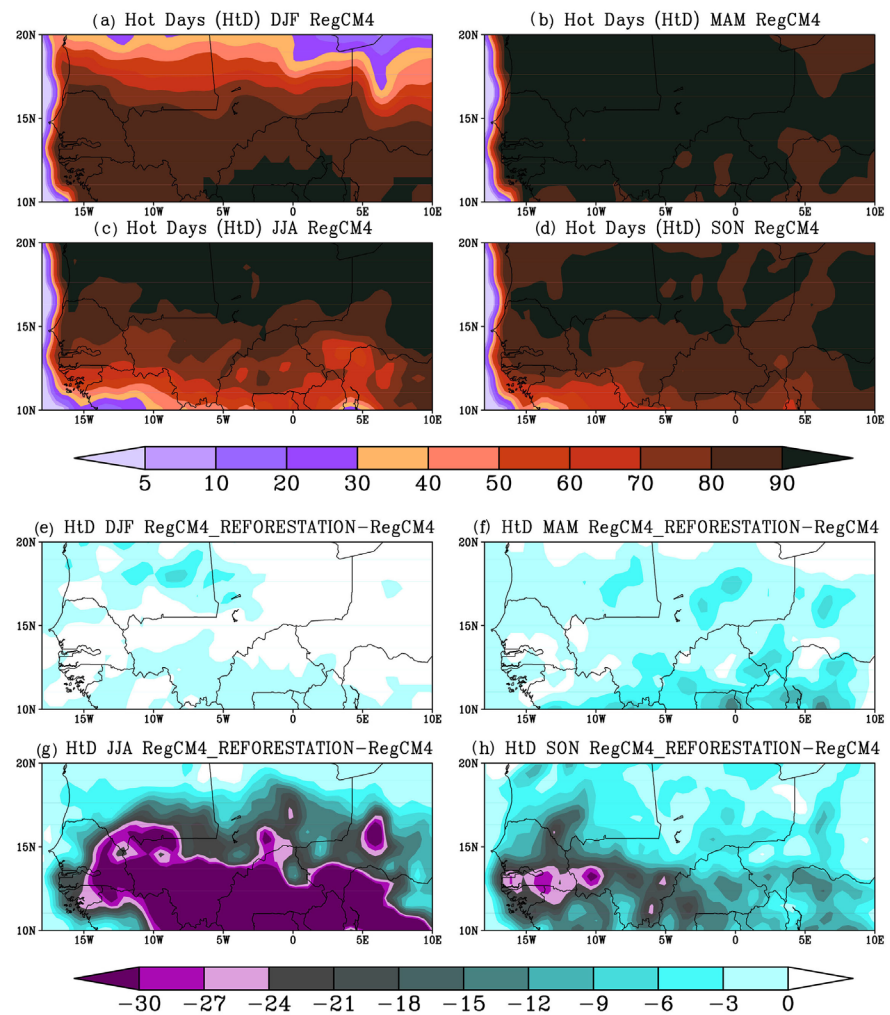


**Figure 12.** Hot days (HtD) averaged from 2003 to 2009 over the Sahel: (top) RegCM4, (down) difference between RegCM4\_REFORESTATION and RegCM4.

the atmospheric moisture content (Figure not shown) over the entire Sahel. Likewise, this decrease is more pronounced during the wet season (JJA).

**Figure 13** shows the seasonal variability of the tropical nights over the Sahel averaged from 2003 to 2009 for the standard version of RegCM4 model (top) and the difference between the two runs (down). The larger tropical nights (>60 days) are recorded over the southern part of the Sahel for the three seasons (DJF, MAM and SON) and over the entire Sahel during JJA. Weak values (<20 days) of this indice are found over the northern part during DJF. The difference between the two runs shows an increase of the TrN over the entire Sahel during DJF and MAM and over the northern part during SON. This could be partly associated to an increase of the surface net downward shortwave flux (**Figure 8**) and the sensible heat flux over the reforested zone (**Figure 5**).

In order to go deeper in the analysis of thermal extremes, the seasonal variability of heat waves days and warm spell days are displayed respectively in **Figure 14** and **Figure 15**. The heat waves days corresponds to the total number of

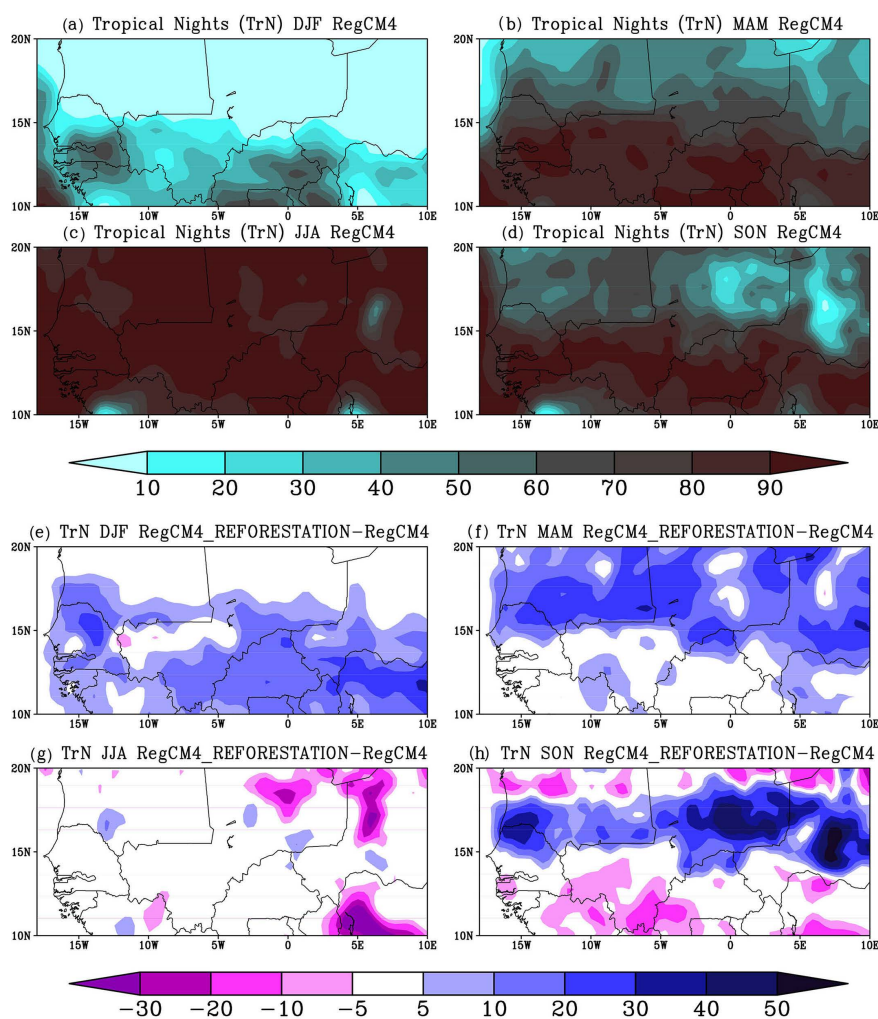


**Figure 13.** Tropical nights (TrN) averaged from 2003 to 2009 over the Sahel: (top) RegCM4, (down) difference between RegCM4\_REFORESTATION and RegCM4.

days of all heat waves events of the study period. When considering the control run, heat waves days mainly occurred over the southern Sahel during JJA and SON periods and over the northern Sahel during the warm season (MAM) (Figure 14). The number of heat waves varies between 2 and 3 per season. This result is consistent with [11] [60]. Studies by [11] showed that from March to May, two to three heat waves propagate eastward over the northern Africa. Low values of heat waves events are found over the northern Sahel during DJF while high values appear over the southern Sahel during JJA. The reforestation tends to increase (decrease) heat waves events over the southern part of the Sahel during JJA and SON periods (over the entire Sahel region during DJF), respectively.

The frequency of warm spell days (WSD) of daily mean temperature is calculated and displayed in Figure 15 for the standard version of RegCM4 model (top) and the difference between the two runs (down) averaged from 2003 to 2009. The standard version of the RegCM4 model simulates longer values (>7 days) of this indice over the Sahel region during DJF period and over the

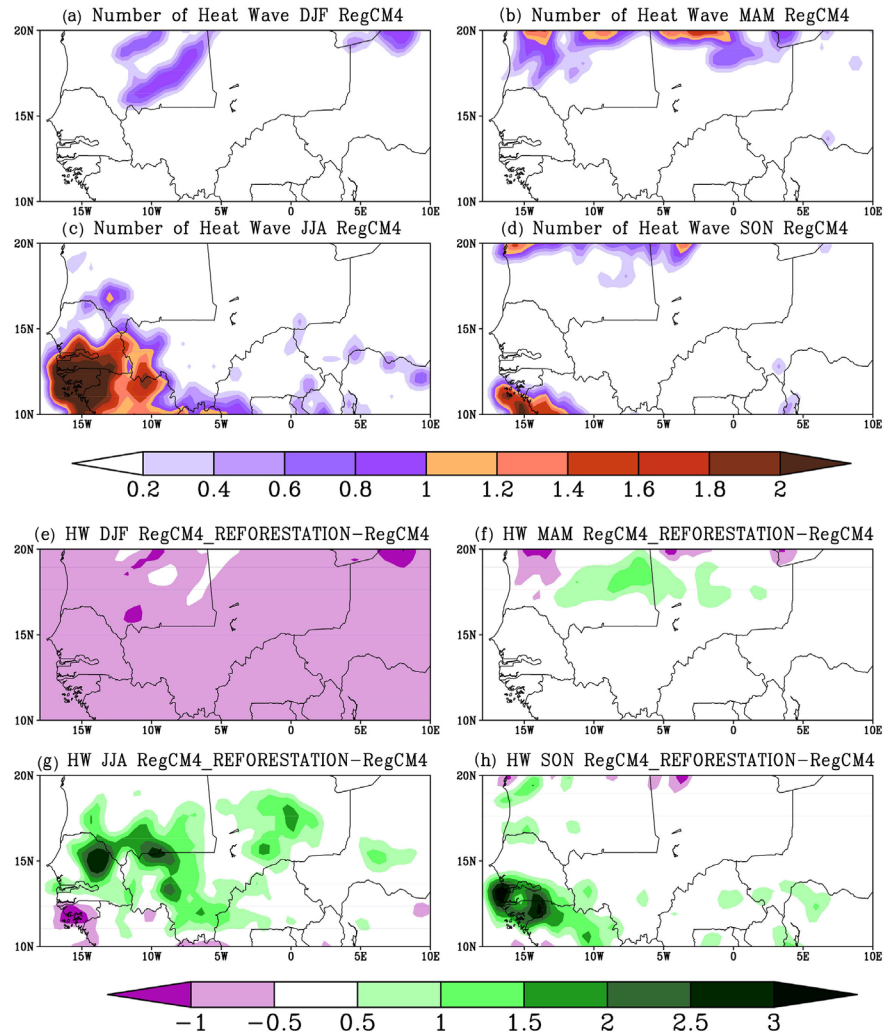


**Figure 14.** Spatial distribution of heat waves days over the Sahel: (top) RegCM4, (down) difference between RegCM4\_REFORESTATION and RegCM4.

Atlantic Ocean during the warm season (MAM) and SON period. Shorter values (<3 days) are found especially over the continent during MAM, JJA and SON. The model simulates shorter values (<2 days) of the frequency of WSD over most part of the coastal regions. When considering the difference between the two versions, a decrease (an increase) of the warm spell days frequency is noticed over the entire Sahel domain during the DJF period (respectively over the Central Sahel during the warm season (MAM) and over the southern Sahel during JJA).

In summary, this study shows that the reforested zone could decrease the warm extremes indices values (TG90P, TX90P and TN90P) over some areas of the Sahel especially during the warm season (MAM) and the summer season (JJA). Nevertheless some Sahelian regions like the eastern part of the Central Sahel could suffer from this land cover change because of the increase of thermal extremes indices.

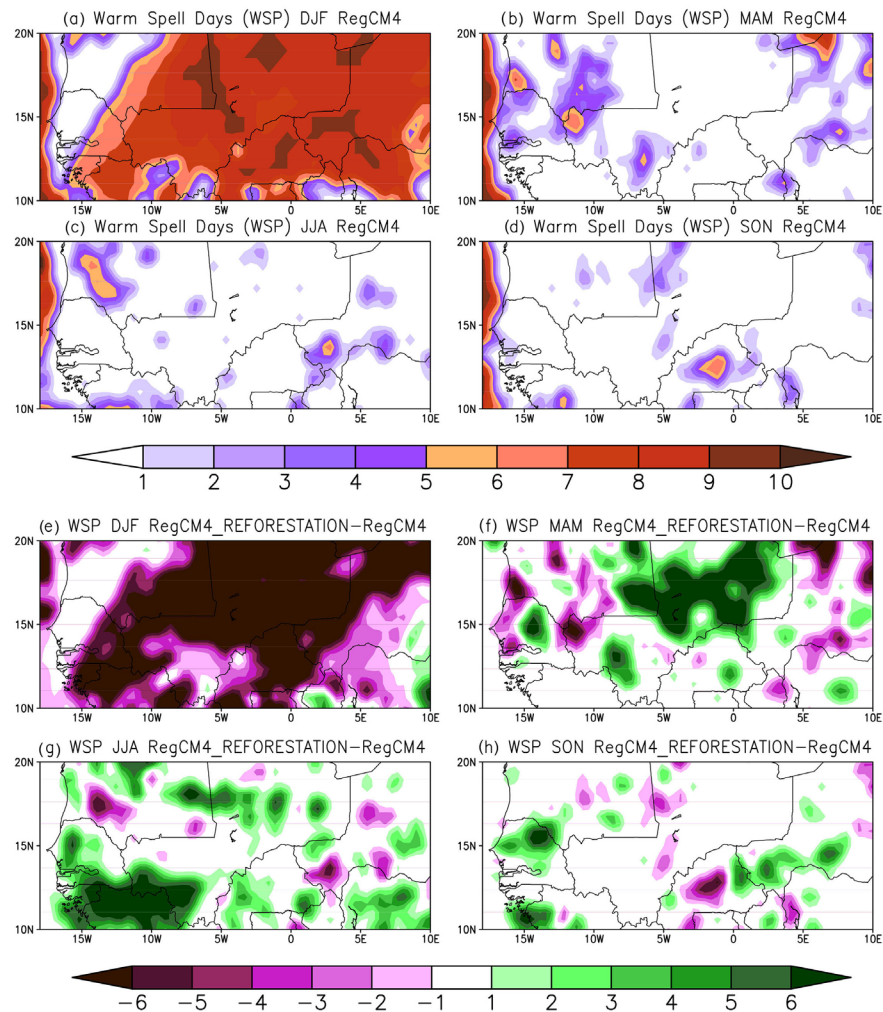


**Figure 15.** Spatial distribution of warm spell days over the Sahel: (top) RegCM4, (down) difference between RegCM4\_REFORESTATION and RegCM4.

#### 4. Conclusions

This work performed two sets of regional climate model experiments (with and without reforestation) to evaluate the impacts of the reforestation of the Sahel-Saharan interface on the seasonal distribution of thermal extremes over the Sahel. The main results of the study are summarized in the following lines.

The reforestation may influence strongly the frequency of warm days (TG90P) by decreasing it over the reforested zone during MAM, the western and eastern Sahel during SON and over the entire Sahel during JJA. The analysis shows a decrease of the frequency of very warm days (TX90P) over the reforested zone during MAM (warm season) and the entire Sahel during JJA (summer season). The TG90P and TX90P indices decrease may be due to an increase of the atmospheric moisture content over the entire Sahel for all seasons and a decrease of the sensible heat flux over the reforested zone. The analysis of the frequency of warm nights (TN90P) shows a decrease over the northern Sahel during DJF, the northern and Central Sahel during MAM, the western and eastern Sahel

during SON and over the entire Sahel during the wet season (JJA).

When considering the variability of hot days, the impact of the reforestation is to decrease them over the entire Sahel for all seasons especially during JJA. This is partly associated to a decrease of the sensible heat flux over the reforested zone and to the strengthening of the atmospheric moisture content over the entire Sahel.

Tropical nights (TrN) are stronger over the southern Sahel during MAM and SON and JJA. The analysis of the difference between the control and the reforested versions shows an increase of the tropical nights over the entire Sahel during DJF and MAM and over the northern Sahel during SON. This may be associated partly to an increase of the surface net downward shortwave flux over the reforested zone.

In order to go deeper in the analysis of extreme thermal indices, heat waves and warm spells indices were analyzed. The heat waves days mainly occurred over the south-west part of the Sahel during JJA when considering the standard version. The reforestation increases the frequency of these events over South Senegal-North Guinea during SON and between North Senegal-South Mauritania during JJA and decreases them over the entire Sahel region during DJF. When considering the warm spell days, the reforestation tends to decrease them over the entire Sahel domain during the DJF period. Changes in latent heat flux appear to be largely responsible for these extreme temperatures variations.

Finally, the results show that the reforestation decreases the warm extremes indices values over some Sahelian regions especially during the warm (MAM) and the summer seasons (JJA) suggesting that this land cover change could have a positive impact on human health particularly over the reforested area. Nevertheless, some Sahel regions like the eastern part of the central Sahel could suffer from this land cover change because of the increase of thermal extremes values. Moreover a study performed by [18] showed that the reforestation may induce an increase of negative effects such as flooding. The results of this study may help the policymakers of the Sahel countries to build efficient strategies to take care of these adverse effects on local populations' socio-economic activities and health.

Despite the results obtained in this work, additional works are needed to better explain the impacts of the reforestation on the seasonal variability of surface temperature and thermal extremes over the Sahel for the present day but also for the near (2050) and far (2100) future using Coupled Model *Intercomparison* Project 5 (CMIP5) climate change projections dynamically downscaled by the RegCM4 model.

## Acknowledgements

The authors would like to thank the Assane SECK University of Ziguinchor, the FIRST program of MESRI-Senegal and the SCAC of the French embassy in Senegal for their support. This study is a part of ANR project ACASIS (2014-2017,

grant: ANR-13-SENV-0007). This work is also partly funded by the NERC/DFID Future Climate for Africa programme under the AMMA-2050 project; grant number NE/M019969/1.

## Conflicts of Interest

The authors declare no conflicts of interest regarding the publication of this paper.

## References

- [1] John, C., Oreskes, N., Doran, P.T., Anderegg, W.R.L., Verheggen, B., Maibach, E., Carlton, J.S., Lewandowsky, S., Skuce, A.G., Green, S.A., Nuccitelli, D., Jacobs, P., Richardson, M., Winkler, B., Painting, R. and Rice, K. (2016) Consensus on Consensus: A Synthesis of Consensus Estimates on Human-Caused Global Warming. *Environmental Research Letters*, **11**, Article ID: 048002.
- [2] IPCC (2013) Summary for Policymakers. Climate Change, 2013. The Physical Science Basis. Contribution of Working Group I to the Fifth Assessment Report of the Intergovernmental Panel on Climate Change. Cambridge University Press, Cambridge, United Kingdom and New York, NY, USA.
- [3] Karl, T.R., Knight, R.W., Gallo, K.P., Peterson, T.C., *et al.* (1993) A New Perspective on Recent Global Warming: Asymmetric Trends of Daily Maximum and Minimum Temperature. *Bulletin of the American Meteorological Society*, **74**, 1007-1023. [https://doi.org/10.1175/1520-0477\(1993\)074<1007:ANPORG>2.0.CO;2](https://doi.org/10.1175/1520-0477(1993)074<1007:ANPORG>2.0.CO;2)
- [4] Easterling, D.R., Horton, B., Jones, P.D., Peterson, T.C., Karl, T.R., Parker, D.E., Salinger, M.J., *et al.* (1997) Maximum and Minimum Temperature Trends for the Globe. *Science*, **277**, 364-367. <https://doi.org/10.1126/science.277.5324.364>
- [5] Easterling, D.R., Meehl, G.A., Parmesan, C., Changnon, S.A., Karl, T.R. and Mearns, L.O. (2000) Climate Extremes: Observations, Modeling and Impacts. *Science*, **289**, 2068-2074. <https://doi.org/10.1126/science.289.5487.2068>
- [6] Coumou, D. and Rahmstorf, S. (2012) A Decade of Weather Extremes. *Nature Climate Change*, **2**, 491-496. <https://doi.org/10.1038/nclimate1452>
- [7] Rome, S., Caniaux, G., Ringard, J., Dieppois, B. and Diedhiou, A. (2015) Identification de tendances récentes et ruptures d'homogénéité des températures : exemple en Afrique de l'Ouest et sur le Golfe de Guinée. Présenté au 28ème colloque international de l'AIC. Liège, Belgique, 591-596.
- [8] Christensen, J.H., Hewitson, B., Busuioc, A., *et al.* (2007) Regional Climate Projections: The Physical Science Basis-Contribution of Working Group 1 to the Fourth Assessment Report of the Intergovernmental Panel on Climate Change. Cambridge University Press, New York, Climate Change.
- [9] Stocker, T.F., Qin, D., Plattner, G.K., Tignor, M., *et al.* (2013) Climate Change. The Physical Science Basis. Working Group I Contribution to the Fifth Assessment Report of the Intergovernmental Panel on Climate Change-Abstract for Decision-Makers. WMO, Geneva, Switzerland, 1552 p.
- [10] Diedhiou, A., Bichet, A., Wartenburger, R., Seneviratne, S.I., Rowell, D.P., Sylla, M.B., Diallo, I., Todzo, S., Touré, N.E., Camara, M., *et al.* (2018) Changes in Climate Extremes over West and Central Africa at 1.5°C and 2°C Global Warming. *Environmental Research Letters*, **13**, Article ID: 065020. <https://doi.org/10.1088/1748-9326/aac3e5>

- [11] Fontaine, B., Janicot, S. and Monerie, P.A. (2013) Recent Changes in Air Temperature, Heat Waves Occurrences and Atmospheric Circulation in Northern Africa. *Journal of Geophysical Research*, **118**, 8536-8552.
- [12] Moron, V., Oueslati, B., Pohl, B., Rome, S. and Janicot, S. (2016) Trends of Mean Temperatures and Warm Extremes in Northern Tropical Africa (1961-2014) from Observed and PPCA-Reconstructed Time Series. *Journal of Geophysical Research: Atmospheres*, **121**, 5298-5319. <https://doi.org/10.1002/2015JD024303>
- [13] Oueslati, B., Pohl, B., Moron, V., Rome, S. and Janicot, S. (2017) Characterisation of Heat Waves in the Sahel and Associated Physical Mechanisms. *Journal of Climate*, **30**, 3095-3115. <https://doi.org/10.1175/JCLI-D-16-0432.1>
- [14] Alo, C.A. and Wang, G. (2010) Role of Vegetation Dynamics in Regional Climate Predictions over Western Africa. *Climate Dynamics*, **35**, 907-922. <https://doi.org/10.1007/s00382-010-0744-z>
- [15] Abiodun, B.J., Pal, J.S., Afiesimama, E.A., Gutowski, W.J. and Adedoyin, A. (2008) Simulation of West African Monsoon Using RegCM3 Part II: Impacts of Deforestation and Desertification. *Theoretical and Applied Climatology*, **93**, 245-261. <https://doi.org/10.1007/s00704-007-0333-1>
- [16] Abiodun, B.J., Adeyewa, Z.D., Oguntunde, P.G., Salami, A.T. and Ajayi, V.O. (2012) Modeling the Impacts of Reforestation on Future Climate in West Africa. *Theoretical and Applied Climatology*, **110**, 77-96. <https://doi.org/10.1007/s00704-012-0614-1>
- [17] Sylla, M.B., Pal, J.S., Wang, G.L. and Lawrence, P.J. (2015) Impact of Land Cover Characterization on Regional Climate Modeling over West Africa. *Climate Dynamics*, **46**, 637-650. <https://doi.org/10.1007/s00382-015-2603-4>
- [18] Diba, I., Camara, M. and Sarr, A.B. (2016) Impacts of the Sahel-Sahara Interface Reforestation on West African Climate: Intra-Seasonal Variability and Extreme Precipitation Events. *Advances in Meteorology*, **2016**, Article ID: 3262451. <https://doi.org/10.1155/2016/3262451>
- [19] Naik, M. and Abiodun, B.J. (2016) Potential Impact of Forestation on the Future Climate Change on Southern Africa. *International Journal of Climatology*, **36**, 4560-4576. <https://doi.org/10.1002/joc.4652>
- [20] Odoulami, R.C., Abiodun, B.J., Ajayi, A.E., Diasso, U.J. and Saley, M.M. (2017) Potential Impacts of Forestation on Heat Waves over West Africa in the Future. *Ecological Engineering*, **102**, 546-556. <https://doi.org/10.1016/j.ecoleng.2017.02.054>
- [21] Balling, R.C. (1988) The Climatic Impacts of a Sonoran Vegetation Discontinuity. *Climatic Change*, **13**, 99-109. <https://doi.org/10.1007/BF00140163>
- [22] Campa, P., Garcia, M., Canton, Y. and Palacios-Orueta, P.-O.A. (2008) Surface Temperature Cooling Trends and Negative Radiative forcing Due to Land Use Change toward Greenhouse Farming in Southeastern Spain. *Journal of Geophysical Research*, **113**, D18109. <https://doi.org/10.1029/2008JD009912>
- [23] Lee, E., Chase, T.N., Rajagopalan, B., Barry, R.G., Biggs, T.W. and Lawrence, P.J. (2009) Effects of Irrigation and Vegetation Activity on Early Indian Summer Monsoon Variability. *International Journal of Climatology*, **29**, 573-581. <https://doi.org/10.1002/joc.1721>
- [24] Feddema, J.J., Oleson, K.W., Bonan, G.B., Mearns, L.O., Buja, L.E., Meehl, G.A. and Washington, W.M. (2005) The Importance of Land-Cover Change in Simulating Future Climates. *Science*, **310**, 1674-1678. <https://doi.org/10.1126/science.1118160>
- [25] Lawrence, P.J., Feddema, J.J., Bonan, G.B., Meehl, G.A., O'Neill, B.C., Oleson, K.W.,

- Levis, S., Lawrence, D.M., Kluzek, E., Lindsay, K. and Thornton, P.E. (2012) Simulating the Biogeochemical and Biogeophysical Impacts of Transient Land Cover Change and Wood Harvest in the Community Climate System Model (CCSM4) from 1850 to 2100. *Journal of Climate*, **25**, 3071-3095.
- [26] Mahmood, R., Pielke Sr., R.A., Hubbard, K.G., DevNiyogi, P.A., Dirmeyer, C.M., Andrew, M., et al. (2014) Land Cover Changes and Their Biogeophysical Effects on Climate. *International Journal of Climatology*, **34**, 929-953.  
<https://doi.org/10.1002/joc.3736>
- [27] Xue, Y., Juang, H.M.H., Li, W., Prince, S., DeFries, R., Jiao, Y. and Vasic, R. (2004) Role of Land Surface Processes in Monsoon Development: East Asia and West Africa. *Journal of Geophysical Research*, **109**, D03105.  
<https://doi.org/10.1029/2003JD003556>
- [28] Zheng, X. and Eltahir, E.A.B. (1998) The Role of Vegetation in the Dynamics of West African Monsoon. *Journal of Climate*, **11**, 2078-2096.  
<https://doi.org/10.1175/1520-0442-11.8.2078>
- [29] Abiodun, B.J., Pal, J., Afiesimama, E.A., Gutowski, W.J. and Adedoyin, A. (2010) Modeling the Impacts of Deforestation on Monsoon Rainfall in West Africa. *IOP Conference Series and Environmental Science*, **13**, Article ID: 012008.  
<https://doi.org/10.1088/1755-1315/13/1/012008>
- [30] Giorgi, F., Coppola, E., Solmon, F., Mariotti, L., Sylla, M.B., Bi, X., et al. (2012) RegCM4: Model Description and Preliminary Tests over Multiple CORDEX Domains. *Climate Research*, **52**, 7-29. <https://doi.org/10.3354/cr01018>
- [31] Grell, G.A., Dudhia, J. and Stauffer, D.R. (1994) Description of the Fifth Generation Penn State/NCAR Mesoscale Model (MM5). Technical Note NCAR/TN-398 + STR, NCAR, Boulder.
- [32] Kiehl, J.T., Hack, J.J., Bonan, G.B., Boville, B.A., Briegleb, B.P., Williamson, D.L. and Rasch, P.J. (1996) Description of the NCAR Community Climate Model (CCM3). NCAR Tech. Note 4201STR, 152.
- [33] Giorgi, F., Mearns, L.O., Shields, C. and McDaniel, L. (1998) Regional Nested Model Simulations of Present Day and  $2 \times \text{CO}_2$  Climate over the Central Plains of the US. *Climatic Change*, **40**, 457-493. <https://doi.org/10.1023/A:1005384803949>
- [34] Dickinson, R.E., Henderson, S.A. and Kennedy, P.J. (1993) Biosphere-Atmosphere Transfer Scheme (BATS) Version 1E as Coupled to the NCAR Community Climate Model. NCAR Tech. rep. TN-387+STR, 72 p.
- [35] Zeng, X., Zhao, M. and Dickinson, R.E. (1998) Intercomparison of Bulk Aerodynamic Algorithms for the Computation of Sea Surface Fluxes Using TOGA COARE and TAO Data. *Journal of Climate*, **11**, 2628-2644.  
[https://doi.org/10.1175/1520-0442\(1998\)011<2628:IOBAAF>2.0.CO;2](https://doi.org/10.1175/1520-0442(1998)011<2628:IOBAAF>2.0.CO;2)
- [36] Pal, J.S., Small, E.E. and Eltahir, E.A.B. (2000) Simulation of Regional Scale Water and Energy Budgets: Representation of Subgrid Cloud and Precipitation Processes within RegCM. *Journal of Geophysical Research*, **105**, 29579-29594.  
<https://doi.org/10.1029/2000JD900415>
- [37] Sylla, M.B., Dell'Aquila, A., Ruti, P.M. and Giorgi, F. (2010) Simulation of the Intraseasonal and the Interannual Variability of Rainfall over West Africa with a RegCM3 during the Monsoon Period. *International Journal of Climatology*, **30**, 1865-1883.
- [38] Mariotti, L., Coppola, E., Sylla, M.B., Giorgi, F. and Piani, C. (2011) Regional Climate Model Simulation of Projected 21st Century Climate Change over an All Africa Domain: Comparison Analysis of Nested and Driving Model Results. *Journal*

- of *Geophysical Research*, **116**, D15111. <https://doi.org/10.1029/2010JD015068>
- [39] Camara, M., Diedhiou, A., Sow, B.A., Diallo, M.D., Diatta, S., Mbaye, I. and Diallo, I. (2013) Analyse de la pluie simulée par les modèles climatiques régionaux de CORDEX en Afrique del'Ouest. *Sécheresse*, **24**, 14-28.
- [40] Holtzlag, A.A.M., et al. (1990) A High Resolution Air Mass Transformation Model for Short-Range Weather Forecasting. *Monthly Weather Review*, **118**, 1561-1575. [https://doi.org/10.1175/1520-0493\(1990\)118<1561:AHRAMT>2.0.CO;2](https://doi.org/10.1175/1520-0493(1990)118<1561:AHRAMT>2.0.CO;2)
- [41] Grell, G.A. (1993) Prognostic Evaluation of Assumptions Used by Cumulus Parameterizations. *Monthly Weather Review*, **121**, 764-787. [https://doi.org/10.1175/1520-0493\(1993\)121<0764:PEOAUB>2.0.CO;2](https://doi.org/10.1175/1520-0493(1993)121<0764:PEOAUB>2.0.CO;2)
- [42] Fritsch, J.M. and Chappell, C.F. (1980) Numerical Prediction of Convectively Driven Mesoscale Pressure Systems. Part I: Convective Parameterization. *Journal of the Atmospheric Sciences*, **37**, 1722-1733. [https://doi.org/10.1175/1520-0469\(1980\)037<1722:NPOCDM>2.0.CO;2](https://doi.org/10.1175/1520-0469(1980)037<1722:NPOCDM>2.0.CO;2)
- [43] Emanuel, K.A. (1991) A Scheme for Representing Cumulus Convection in Large-Scale Models. *Journal of the Atmospheric Sciences*, **48**, 2313-2335.
- [44] Simmons, A.S., Uppala, D. and Kobayashi, S. (2007) ERA-Interim: New ECMWF Reanalysis Products from 1989 Onwards. *ECMWF Newsletter*, **110**, 29-35.
- [45] Uppala, S., Dee, D., Kobayashi, S., Berrisford, P. and Simmons, A. (2008) Towards a Climate Data Assimilation System: Status Update of ERA-Interim. *ECMWF Newsletter*, **115**, 12-18.
- [46] Jones, P.D. (2014) Climatic Research Unit (CRU) Time-Series (TS) Version 3.22 of High Resolution Gridded Data of Month-by-Month Variation in Climate (Jan. 1901-Dec. 2013) University of East Anglia. NCAS British Atmospheric Data Centre.
- [47] Kothe, S. and Ahrens, B. (2010) On the Radiation Budget in Regional Climate Simulations for West Africa. *Journal of Geophysical Research*, **115**, D23120. <https://doi.org/10.1029/2010JD014331>
- [48] Oettli, P., Sultan, B., Baron, C. and Vrac, M. (2011) Are Regional Climate Models Relevant for Crop Yield Prediction in West Africa? *Environmental Research Letter*, **6**, Article ID: 014008. <https://doi.org/10.1088/1748-9326/6/1/014008>
- [49] Paeth, H., Hall, N.M., Gaertner, M.A., et al. (2011) Progress in Regional Downscaling of West African Precipitation. *Atmospheric Science Letters*, **12**, 75-82. <https://doi.org/10.1002/asl.306>
- [50] Diallo, I., Sylla, M.B., Camara, M. and Gaye, A.T. (2013) Interannual Variability of Rainfall over the Sahel Based on Multiple Regional Climate Models Simulations. *Theoretical and Applied Climatology*, **113**, 351-362. <https://doi.org/10.1007/s00704-012-0791-y>
- [51] Dee, D.P., Uppala, S.M., Simmons, A.J., et al. (2011) The ERA-Interim Reanalysis: Configuration and Performance of the Data Assimilation System. *Quarterly Journal of the Royal Meteorology Society*, **137**, 553-597.
- [52] Diallo, I., Bain, C.L., Gaye, A.T., Moufouma-Okia, W., Niang, C., Dieng, M.D.B. and Graham, R. (2014) Simulation of the West African Monsoon Onset Using the HadGEM3-RA Regional Climate Model. *Climate Dynamics*, **43**, 575-594. <https://doi.org/10.1007/s00382-014-2219-0>
- [53] Peterson, T.C., Folland, C., Gruza, G., Hogg, W., et al. (2001) Report on the Activities of the Working Group on Climate Change Detection and Related Rapporteurs 1998-2001. WMO Rep. WCDMP 47, WMO-TD 1071, Geneva.
- [54] Hagos, S.M. and Cook, K.H. (2007) Dynamics of the West African Monsoon Jump.

---

*Journal of Climate*, **20**, 52-64. <https://doi.org/10.1175/2007JCLI1533.1>

- [55] Thorncroft, C.D., Nguyen, H., Zhang, C. and Peyrillé, P. (2011) Annual Cycle of the West African Monsoon: Regional Circulations and Associated Water Vapour Transport. *Quarterly Journal of the Royal Meteorology Society*, **137**, 129-147.
- [56] Mohr, K.I. and Thorncroft, C.D. (2006) Intense Convective Systems in West Africa and Their Relationship to the African Easterly Jet. *Quarterly Journal of the Royal Meteorological Society*, **132**, 163-176. <https://doi.org/10.1256/qj.05.55>
- [57] Steiner, A.L., Pal, J.S., Rauscher, S.A., Bell, J.L., Diffenbaugh, N.S., Boone, A., Sloan, L.C. and Giorgi, F. (2009) Land Surface Coupling in Regional Climate Simulations of the West African Monsoon. *Climate Dynamics*, **33**, 869-892. <https://doi.org/10.1007/s00382-009-0543-6>
- [58] Sylla, M.B., Giorgi, F. and Stordal, F. (2012) Origins of Rainfall and Temperature Bias in High Resolution Simulations over Southern Africa. *Climate Research*, **52**, 193-211.
- [59] Konaré, A., Zakey, A.S., Solmon, F., Giorgi, F., Rauscher, S., Ibrah, S. and Bi, X. (2008) A Regional Climate Modeling Study of the Effect of Desert Dust on the West African Monsoon. *Journal of Geophysical Research*, **113**, D12206. <https://doi.org/10.1029/2007JD009322>
- [60] Rome, S., Oueslati, B., Moron, V., Pohl, B. and Diedhiou, A. (2016) Les vagues de chaleur au Sahel: Définition et principales caractéristiques spatio-temporelles (1973-2014). *Actes du IXXXème colloque de l'Association Internationale de Climatologie*, Besançon, 6-9 juillet 2016, 345-350.